

# A $\alpha$ -cyanostilbene-modified Schiff base as efficient turn-on fluorescent chemosensor for $\text{Zn}^{2+}$

AIXIANG DING<sup>a</sup>, FANG TANG<sup>a</sup>, TAO WANG<sup>a</sup>, XUTANG TAO<sup>b</sup> and JIAXIANG YANG<sup>a,b,\*</sup>

<sup>a</sup>Department of Chemistry, Key Laboratory of Functional Inorganic Materials of Anhui Province, Anhui University, Hefei 230039, P. R. China

<sup>b</sup>State Key Laboratory of Crystal Materials, Shandong University, Jinan, Shandong 250100, P. R. China  
e-mail: jxyang@ahu.edu.cn

MS received 5 May 2014; revised 14 June 2014; accepted 9 July 2014

**Abstract.** A novel Schiff base derivative (Z)-3-(4-(hexyloxy)phenyl)-2-(4-((E)-2-hydroxybenzylidene amino)phenyl)acrylonitrile (**L**) was designed, synthesized and characterized. **L** was used as a  $\text{Zn}^{2+}$  selective, turn-on, fluorescent chemosensor with a detection limit of 0.1  $\mu\text{M}$  in DMF. 1:1 stoichiometric complex formation of **L** with  $\text{Zn}^{2+}$  was confirmed through fluorescent titration experiments and Job's plot. The enhancement of fluorescence intensity of **L** with addition of  $\text{Zn}^{2+}$  is the consequence of the inhibited isomerization of the C=N bond, namely chelation-enhanced fluorescence (CHEF) effect.

**Keywords.** Fluorescence sensor; Schiff base;  $\alpha$ -cyanostilbene; chelation-enhanced fluorescence effect; zinc ion.

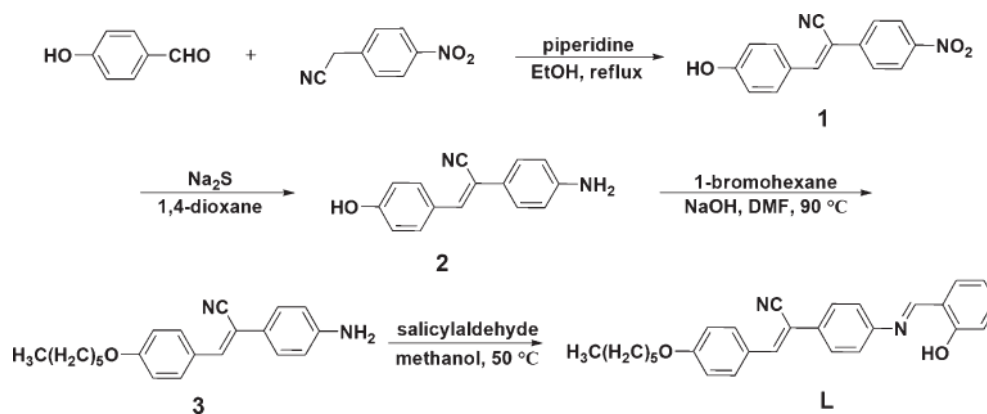
## 1. Introduction

Metal ions are essential for all forms of life because of their vitally important role in fundamental processes.<sup>1</sup> As the second most abundant transition metal ion after iron in the human body,  $\text{Zn}^{2+}$  plays significant role in a number of biological processes such as gene expression, enzyme regulation, neural signal transmission and cell apoptosis, to name a few.<sup>2–4</sup> Therefore, development of novel fluorescent sensors for  $\text{Zn}^{2+}$  in the presence of a variety of other metal ions has received considerable attention.<sup>5–13</sup> Recently, progress in the area of turn-on and/or ratiometric chemosensors has contributed significantly to the development of a variety of  $\text{Zn}^{2+}$  probes based on fluorescein, coumarin, anthracene, carbazole, quinoline, cyanine dyes, rhodamine, naphthalimide, pyrene, BODIPY, etc.<sup>14–20</sup> Despite the fact that some of them were excellent for  $\text{Zn}^{2+}$  sensing, their structures are complicated and require multi-step and inefficient synthetic methods.<sup>21–23</sup> In addition, it is still a challenge to design excellent  $\text{Zn}^{2+}$  probes to overcome the difficulty in distinguishing  $\text{Zn}^{2+}$  from  $\text{Cd}^{2+}$  due to their similar properties.<sup>8,24,25</sup> Keeping this in mind, it is imperative to design new probes which are endowed with sensitivity, selectivity and simplicity.

Schiff base derivatives are known to be superior ligands for transition metal ions,<sup>26–28</sup> and numerous Schiff base metal complexes showed anti-tumour behaviour, anti-oxidative activity and anti-microbial property.<sup>29–31</sup> Recently, Schiff base derivatives were used as chemosensors which attracted much attention due to the simplicity of synthetic methods, high efficiency, high selectivity, excellent applicability, and so forth.<sup>32–37</sup> Schiff base derivatives combined with  $\pi$ -conjugated fluorescent moiety are especially fascinating tools in the optical sensing for metal ions.<sup>38–40</sup>  $\alpha$ -Cyanostilbene derivatives were deeply studied and widely used as fluorescent sensors in recent years,<sup>41–43</sup> but there are very few reports focused on the metal ion sensors. Given the outstanding fluorescent properties of  $\alpha$ -cyanostilbene derivatives<sup>44–47</sup> and the strong binding ability of salicylidene Schiff base to metal ions,<sup>48</sup> we describe herein a novel salicylidene Schiff base functionalized with  $\alpha$ -cyanostilbene moiety, which was expected to bind with  $\text{Zn}^{2+}$  and give effective fluorescence enhancement. To some extent, this kind of strategy would be instructive for new-type fluorescence probes of metal ions.

In our present work, a newly designed and synthesized Schiff base, (Z)-3-(4-(hexyloxy)phenyl)-2-(4-((E)-2-hydroxybenzylideneamino)phenyl)acrylonitrile (**L**, scheme 1), was used as an efficient and user-friendly 'turn-on' chemosensor for specific recognition of  $\text{Zn}^{2+}$  with the ability to distinguish  $\text{Zn}^{2+}$  from  $\text{Cd}^{2+}$ .

\*For correspondence



Scheme 1. Synthesis of probe L.

## 2. Experimental

### 2.1 Materials and instrumentation

All chemicals were purchased from Sigma Aldrich and used without further purification.  $^1\text{H}$  NMR and  $^{13}\text{C}$  NMR were recorded on a Bruker Avance 400 MHz NMR spectrometer. Both  $^1\text{H}$  and  $^{13}\text{C}$  NMR were used for tetramethylsilane ( $\text{SiMe}_4$ ) as internal standards. NMR data were reported as follows: chemical shifts ( $\delta$ ) in ppm, multiplicity (s = singlet, d = doublet, t = triplet, m = multiplet), coupling constants  $J$  (Hz), integration, and interpretation. UV-Vis absorption spectra were recorded on a TU-1901 of Beijing Purkinje General Instrument Co., Ltd, spectrometer with quartz cuvettes of 1.0 cm path length. Fluorescence spectra were recorded on a Shimadzu RF 5301 PC fluorescence spectrometer using samples in solution. FT-IR spectra were obtained in KBr discs on a Nicolet 380 FT-IR spectrometer in the 4000–400  $\text{cm}^{-1}$  region. Fluorescence images were obtained using a digital camera (Nikon D7000).

### 2.2 Synthesis

**2.2a The synthesis of (Z)-3-(4-hydroxyphenyl)-2-(4-nitrophenyl)acrylonitrile (1):** The synthetic route of **1** according to the reported procedure<sup>49</sup> was modified. 4-Hydroxybenzaldehyde and 4-nitrobenzylcyanide was dissolved in EtOH at 78 °C. Then two drops of piperidine were added. After 4 h, the mixture was cooled to room temperature and a precipitate was formed. The product was hot filtered and dried in vacuo at 60 °C to give a purple solid with a yield of 93%.

**2.2b The synthesis of (Z)-2-(4-aminophenyl)-3-(4-hydroxyphenyl)acrylonitrile (2):** The synthetic route

for compound **2** was reported in our previous publication.<sup>50</sup> FT-IR (KBr,  $\text{cm}^{-1}$ ): 3434 (vs), 3341 (vs), 3285 (vs), 2215 (m), 1793 (w), 1624 (m), 1605 (vs), 1521 (vs), 1447 (m), 1400 (m), 1281 (m), 1258 (s), 1179 (s), 890 (w), 825 (m).  $^1\text{H}$  NMR ( $\text{CDCl}_3$ , 400 MHz):  $\delta$  10.02 (s, 1 H, OH), 7.75 (d, 2 H, ArH,  $J = 8.8$  Hz), 7.54 (s, 1 H, CH), 7.36 (d, 2 H, ArH,  $J = 8.4$  Hz), 6.66 (d, 2 H, ArH,  $J = 8.8$  Hz), 6.62 (d, 2 H, ArH,  $J = 8.8$  Hz), 5.42 (s, 2 H,  $\text{NH}_2$ ).  $^{13}\text{C}$  NMR ( $\text{CDCl}_3$ , 400 MHz):  $\delta$  158.9, 149.5, 137.1, 130.5, 137.1, 129.7, 128.3, 125.4, 121.3, 118.9, 115.7, 115.6, 105.8.

**2.2c The synthesis of (Z)-2-(4-aminophenyl)-3-(4-(hexyloxy)phenyl)acrylonitrile (3):** A mixture of compound **2** (1 g, 4.23 mmol) dissolved in DMF (10 mL) and NaOH (271 mg, 6.78 mmol) was stirred for 15 min at RT. Then 1-bromohexane (928.8 mg, 8.47 mmol) was added, and the mixture was sequentially stirred for 12 h at 90 °C. The mixture was poured into 500 mL water and extracted with ethyl acetate ( $3 \times 100$  mL) three times. Finally, after silica gel column chromatography (n-hexane: EtOAc = 3:1), the product was recrystallized from ethanol and water to give a yellow powder with a yield of 69.7% (945.18 mg, 2.95 mmol). FT-IR (KBr,  $\text{cm}^{-1}$ ): 3459 (vs), 3364 (vs), 3029 (s), 2954 (s), 2923 (s), 2867 (s), 2211 (m), 1795 (m), 1606 (vs), 1516 (vs), 1465 (s), 1397 (s), 1297 (s), 1257 (s), 1177 (s), 1027 (m), 897 (m), 872 (m), 833 (w), 712 (m), 666 (w).  $^1\text{H}$  NMR ( $\text{CDCl}_3$ , 400 MHz, ppm):  $\delta$  7.80 (d, 2 H, ArH,  $J = 8.8$  Hz), 7.44 (d, 2 H, CH,  $J = 8.4$  Hz), 7.29 (s, 1 H, ArH), 6.93 (d, 2 H, ArH,  $J = 8.8$  Hz), 6.70 (d, 2 H, ArH,  $J = 8.4$  Hz), 5.29 (s, 2 H,  $\text{NH}_2$ ), 3.99 (t, 2 H,  $\text{CH}_2$ ), 1.79 (m, 2 H,  $\text{CH}_2$ ), 1.46 (m, 2 H,  $\text{CH}_2$ ), 1.35 (t, 4 H,  $\text{CH}_2$ ), 0.91 (t, 3 H,  $\text{CH}_3$ ).  $^{13}\text{C}$  NMR ( $\text{CDCl}_3$ , 400 MHz, ppm):  $\delta$  160.5, 147.1, 138.5, 130.7, 127.0, 126.8, 125.0, 118.9, 115.1, 114.8, 108.6, 68.2, 53.5, 31.6, 29.1, 25.7, 22.6, 14.1.

**2.2d The synthesis of compound L:** In a 50 mL round bottom flask, compound **3** (200 mg, 0.625 mmol) was dissolved in 12.0 mL hot methanol and heated to 50°C in an oil bath. Then, salicylaldehyde (91.5 mg, 0.750 mmol) and two drops HOAc were added into the flask, the mixture was heated to 55°C for 12 h. Finally, the orange-yellow precipitate was filtered, dried and obtained with a yield of 66.4% (176 mg). FT-IR (KBr,  $\text{cm}^{-1}$ ): 3441 (m), 3055 (w), 2921 (s), 2852 (m), 2215 (w), 1598 (vs), 1580 (w), 1513 (m), 1455 (w), 1259 (s), 1180 (s), 1028 (w), 835 (m), 756 (m), and 535 (w).  $^1\text{H}$  NMR ( $\text{CDCl}_3$ , 400 MHz, ppm): 13.09 (s, 1 H, OH), 8.62 (s, 1 H, CH), 7.87 (d, 2 H, ArH,  $J = 8.4$  Hz), 7.68 (d, 2 H, ArH,  $J = 8.4$  Hz), 7.44 (s, 1 H, CH), 7.38 (t, 2 H, ArH), 7.31 (d, 2 H, ArH,  $J = 8.8$  Hz), 6.95 (d, 1 H, ArH,  $J = 7.6$  Hz), 6.94–6.92 (m, 3 H, ArH), 3.99 (t, 3 H,  $\text{CH}_2$ ), 1.79 (m, 2 H,  $\text{CH}_2$ ), 1.46 (m, 2 H,  $\text{CH}_2$ ), 1.34 (m, 4 H,  $\text{CH}_2$ ), 0.91 (t, 3 H,  $\text{CH}_3$ ).  $^{13}\text{C}$  NMR ( $\text{CDCl}_3$ , 400 MHz, ppm): 162.9, 161.2, 148.6, 141.7, 133.6, 132.6, 131.3, 126.8, 126.1, 121.9, 119.2, 119.1, 118.6, 117.3, 107.6, 68.3, 31.6, 29.1, 26.7, 22.6 and 14.1.

### 2.3 Fluorescent measurements

Stock solutions (10 mM) of **L** and the mineral salts ( $\text{Cd}^{2+}$ ,  $\text{Ba}^{2+}$ ,  $\text{K}^+$ ,  $\text{Ni}^{2+}$ ,  $\text{Pb}^{2+}$ ,  $\text{Zn}^{2+}$ , etc.) were prepared in DMF and methanol, respectively. Test solutions were prepared by placing 5  $\mu\text{L}$  of the probe stock solution into a volumetric flask, adding an appropriate aliquot of stock solutions of each ion, and diluting the solutions into 5 mL with DMF solvent. Spectral bandwidth of both excitation and emission monochromators was 5 nm.

## 3. Results and Discussion

### 3.1 The preliminary confirmation for the detection of $\text{Zn}^{2+}$

Firstly, the qualitative estimation of the selectivity of the chemosensor **L** towards different cations was performed under UV 365 nm light (figure 1). The

luminescence changes were easily monitored. Obviously, colour changes were observed from colourless to green when  $\text{Zn}^{2+}$  ions were added to the solutions of **L** (10  $\mu\text{M}$ ) under UV 365 nm light. Conversely, there were no noticeable changes after adding a large excess of other metal ions. These results implied a formation of new complex between  $\text{Zn}^{2+}$  and **L**, and the complex showed a totally different property from that of **L**. Hence, distinct luminescence changes were observed.

### 3.2 Spectral studies for the solvent effects toward **L** and **L-Zn** $^{2+}$

It is well known that the solvents play significant roles in the optical properties of **L** and its binding abilities with different metal ions. Therefore, corresponding optical tests in various solvents were conducted under the concentration of 10  $\mu\text{M}$ . As shown in figure 2a, the absorptions change little with the increase of solvent polarity. However, a dramatically bathochromic shift effect occurred from 430.6 nm (benzene) to 532 nm (DMF) in the fluorescence spectra due to the large internal charge transfer (ICT, charge transferred from the alkoxy phenyl ring and amino phenyl ring to the acrylonitrile moiety) process involved in **L** (figure 2b). Besides, the effect of different solvents on **L** toward  $\text{Zn}^{2+}$  sensing was also studied. It was observed that there was a significant enhancement in the fluorescence intensity by addition of  $\text{Zn}^{2+}$  into the DMF solutions of **L**. Therefore, DMF would be the suitable solvent for the comprehension of the sensitive, selective and binding properties of probe **L** with  $\text{Zn}^{2+}$ . Whereas, there was only a slight change in the other solvents except for EtOH. The experimental data indicate that the properties of the solvents, such as protic property and polarity, markedly affect binding ability and the fluorescence intensity of **L** with  $\text{Zn}^{2+}$ .

### 3.3 UV-Vis absorption and fluorescence titration

The UV-Vis absorption response of **L** with gradual addition of  $\text{Zn}^{2+}$  in DMF was investigated (figure 3a).

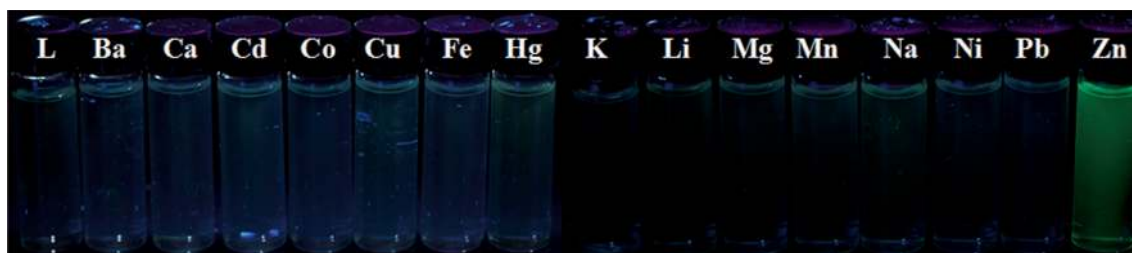


**Figure 1.** Luminescence responses of probe **L** (10  $\mu\text{M}$ ) to the addition of different cations in DMF solutions under the UV 365 nm light.

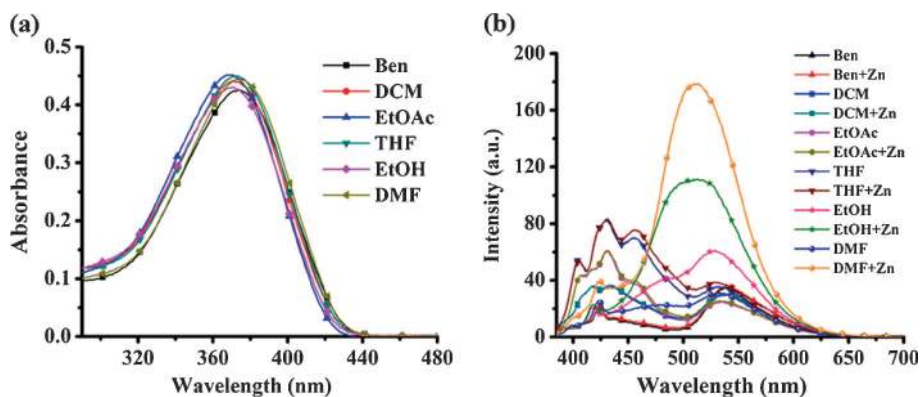


**Figure 2.** (a) UV-Vis spectra of **L** ( $10\ \mu\text{M}$ ) and (b) fluorescence emission spectra of **L** and **L-Zn<sup>2+</sup>** in benzene, DCM, EA, THF, EtOH, and DMF.

From the curves, we can see that **L** showed a main absorption band at 373 nm in the absence of  $\text{Zn}^{2+}$ . With the gradual increase of  $\text{Zn}^{2+}$  concentrations, the absorbance band at 373 nm gradually decreased in intensity with a slight blue shift. And two new absorption bands appeared at 296 and 438 nm with two isosbestic points at 335 and 410 nm, indicating a formation of stable complex between **L** and  $\text{Zn}^{2+}$ . The fluorescence spectra of **L** and its titration experiments were recorded by adding various amounts of zinc ions to the solution containing a constant concentration of **L**. Figure 3b shows the fluorescence spectra upon addition of various concentrations of  $\text{Zn}^{2+}$  in DMF, which were recorded at an excitation wavelength of 370 nm and emission wavelength of 380–680 nm. Initially, probe **L** showed a very weak spectrum due to the result of the isomerization of C=N double bond. The emission intensity enhanced gradually along with the gradual increase of concentration of  $\text{Zn}^{2+}$ . The evident enhancement in the fluorescence intensity was ascribed to the inhibited C=N isomerization. The fluorescence

emission at 507 nm reached maximum value after addition of 1 equiv. of  $\text{Zn}^{2+}$ . It indicates that 1:1 stoichiometry is most possible for the binding mode of **L** with  $\text{Zn}^{2+}$ .

### 3.4 Application studies

As a fluorescence probe, it must have a highly selective performance to the specified ion over the other potential interfering ions. Selective experiments were performed to investigate the effect of other competitive metal ions on the fluorescence spectra, including heavy, alkali earth and transition metal ions such as  $\text{Ba}^{2+}$ ,  $\text{Cd}^{2+}$ ,  $\text{Co}^{2+}$ ,  $\text{Cu}^{2+}$ ,  $\text{Fe}^{2+}$ ,  $\text{K}^+$ ,  $\text{Li}^+$ ,  $\text{Mg}^{2+}$ ,  $\text{Mn}^{2+}$ ,  $\text{Na}^+$ ,  $\text{Ni}^{2+}$ , and  $\text{Pb}^{2+}$ . As shown in figure 4, addition of  $\text{Zn}^{2+}$  resulted in evident fluorescence enhancement, but little changes could be observed with the interfering metal ions. Most importantly, the probe **L** distinguished  $\text{Zn}^{2+}$  from  $\text{Cd}^{2+}$ , a frequently encountered trouble in the design for the  $\text{Zn}^{2+}$  fluorescent probes. Furthermore, we conducted the competition experiments by adding

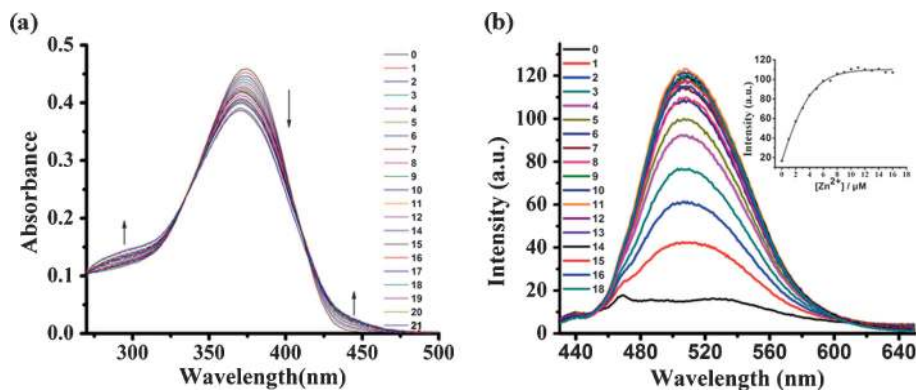


**Figure 3.** (a) UV-Vis absorption spectra of **L** ( $10\ \mu\text{M}$ ) obtained during the titration by  $\text{Zn}(\text{NO}_3)_2$  (0 ~ 20: 0–20  $\mu\text{M}$ , 21: 30  $\mu\text{M}$ .) in DMF at room temperature. (b) Fluorescent emission spectra of **L** ( $10\ \mu\text{M}$ ) in the presence of different concentrations of  $\text{Zn}^{2+}$  in DMF. Excitation wavelength was at 370 nm. Inset: the fluorescent intensity as a function of  $\text{Zn}^{2+}$  concentration.

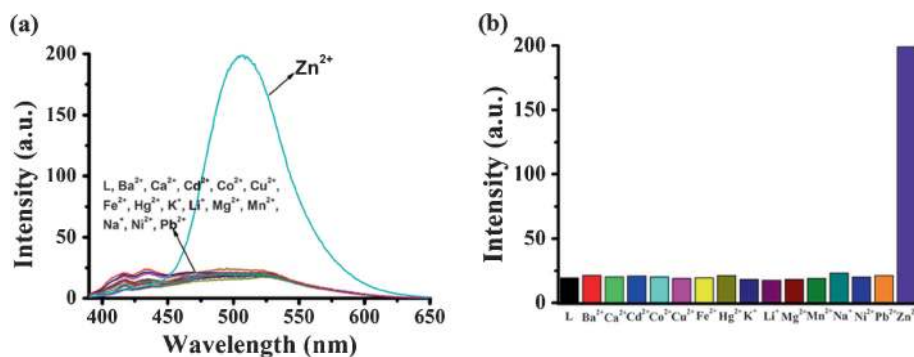


**Figure 4.** (a) Fluorescence spectra of **L** ( $10\ \mu\text{M}$ ) in the absence (ion-free) and presence of 1 equiv. of different metal ions in DMF under 370 nm UV excitation. (b) Fluorescent intensity of **L** at 509 nm upon addition of different cations.

excess above-mentioned metal ions to the solutions of **L** in the presence of  $\text{Zn}^{2+}$ . As shown in figure 5, the ratios of  $I_M^{n+}/I_{\text{Zn}^{2+}}$  deduced from other cations are similar to that of only  $\text{Zn}^{2+}$  in the solution. These results reveal that **L** can serve as an excellent selective fluorescent chemosensor for  $\text{Zn}^{2+}$ .

### 3.5 Job's plot and Benesi-Hilderand plot

To further determine a binding mode and the detection limit, Job's and Benesi-Hildebrand plot analysis were conducted (figure 6). Job's plot showed that when the  $\text{Zn}^{2+}$  molar fraction reaches 0.5, the maximum fluorescence emission intensity is obtained, indicating a 1:1 binding model between **L** and  $\text{Zn}^{2+}$ . On the basis of 1:1 stoichiometry, the binding ratio and stability constant of the complex between **L** and  $\text{Zn}^{2+}$  was estimated to be

$0.994$  and  $2.317 \times 10^5\ \text{M}^{-1}$  by plotting  $1/\Delta F$  against  $1/[\text{Zn}^{2+}]$  according to the Benesi-Hilderbrand equation, which demonstrated a powerful binding ability of **L** with  $\text{Zn}^{2+}$ . Meanwhile, the limit detected concentration of  $\text{Zn}^{2+}$  is determined to be  $0.1\ \mu\text{M}$  in DMF.

### 3.6 Exploration for practical application

Application in practical environment is very important and prerequisite for a novel fluorescence sensor. To explore the application value in practical setting, **L** towards  $\text{Zn}^{2+}$  sensing in different water fraction was studied (figure 7a). Compared with that in pure DMF solution, the fluorescence emission were very weak in the mixed water/DMF (v/v) solutions of 10, 20, 80, 90 and 100%. However, it is noted that it still had a relative intensive fluorescence emission in the water range

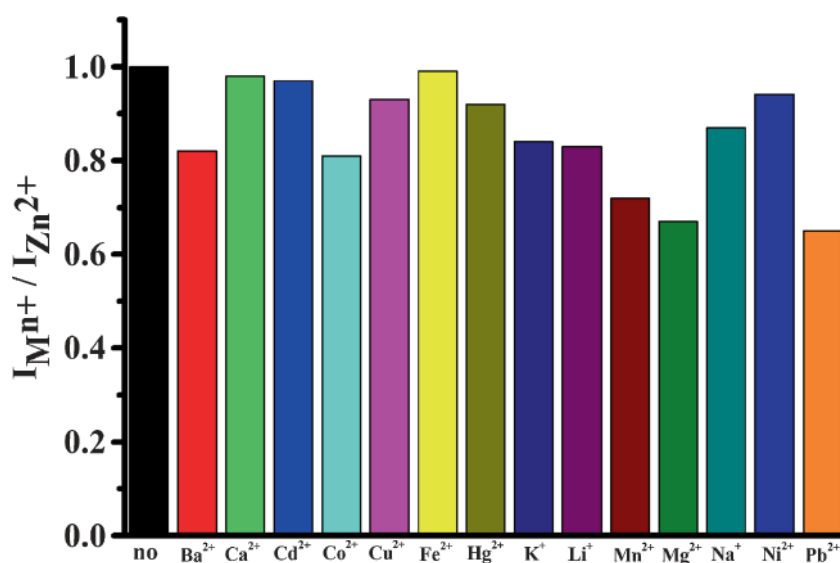


**Figure 5.** Fluorescent response of ligand  $10\ \mu\text{M}$  **L** containing  $10\ \mu\text{M}$   $\text{Zn}^{2+}$  in presence of selected metal ions ( $100\ \mu\text{M}$ ). Excitation was at 370 nm and the emission was at 509 nm.

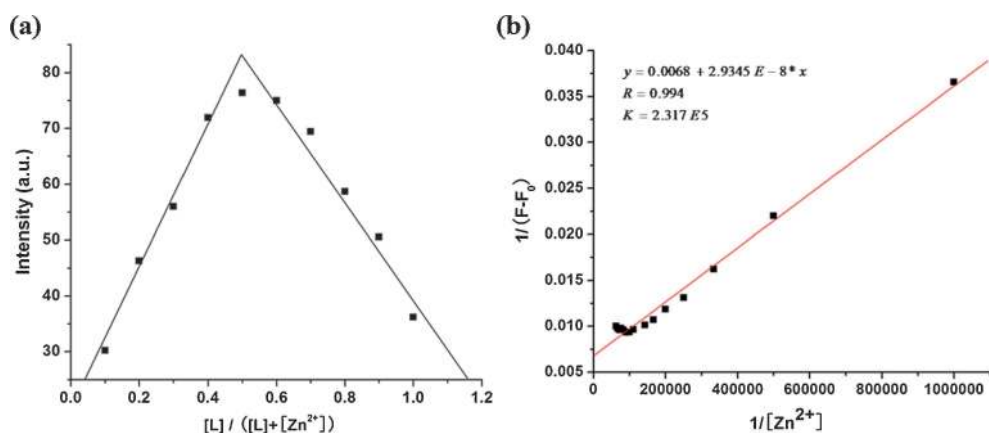


**Figure 6.** (a) Job's plot of complexation between **L** and  $Zn^{2+}$  ( $\lambda_{ex} = 370$  nm). The total concentrations of **L** and  $Zn^{2+}$  are  $10 \mu M$ . The experiments were conducted at room temperature in DMF. (b) Benesi-Hildebrand plot of the **L**- $Zn^{2+}$  complexation in DMF solution. X-axis unit is in  $M^{-1}$ .

of 30–70%, and even showed a stronger emission when water fraction reached 40 and 50%. Hence probe **L** can be availablely used as  $Zn^{2+}$  chemosensor in a quite wide water fraction range. Also appropriate pH condition for a probe to its detected metal ions is essential. The figure S1 and 7b showed the fluorescence emission intensity of **L** at various pH values with addition of 1 equiv.  $Zn^{2+}$  to its DMF/HEPES (v/v, 1/1) mixed solutions. Over a pH range of 6–12, probe **L** showed a good response to  $Zn^{2+}$ . At pH 1 ~ 5, the fluorescence showed weak intensity and declined slowly with the decrease of pH. It indicates that the sensing behaviours of **L** towards  $Zn^{2+}$  is effective in alkaline, neutral and faintly acid conditions.

### 3.7 The mechanism for the fluorescence enhancement

To gain an insight to the fluorescence behaviour of probe **L** and its chelation complex **L**- $Zn^{2+}$ , DFT and TDDFT calculations were carried out.<sup>51</sup> According to

the above experimental and analyzed results, we speculated a reasonable binding mode: a four coordinated single nuclear complex between **L** and  $Zn^{2+}$  (figure S2). The optimized structure was obtained using a suite of Gaussian 09 package adopting B3LYP method under the 6-31G\* basic set. TDDFT calculations were performed to get the excitation energies and oscillator strengths (table S1). The electron clouds of the HOMO levels for the probe **L** distribute in a quite wide range, from the salicylaldehyde part to the cyanostilbene moiety, whereas the LUMO focused on the cyanoethylene moiety. Hence an intrinsic ICT was endowed by such electronic distributions. Unlike the probe **L**, the electronic clouds of the HOMO and LUMO levels for the complex **L**- $Zn^{2+}$  both lied on the  $\pi$ -conjugated system, thus leading to a broken ICT effect when the Schiff base derivative coordinated with  $Zn^{2+}$ . The ICT in probe **L** is responsible for the large red shift in high polar solvents and the forbidden ICT in the complex **L**- $Zn^{2+}$  is the reason of the slight blue shift in the UV-Vis titration

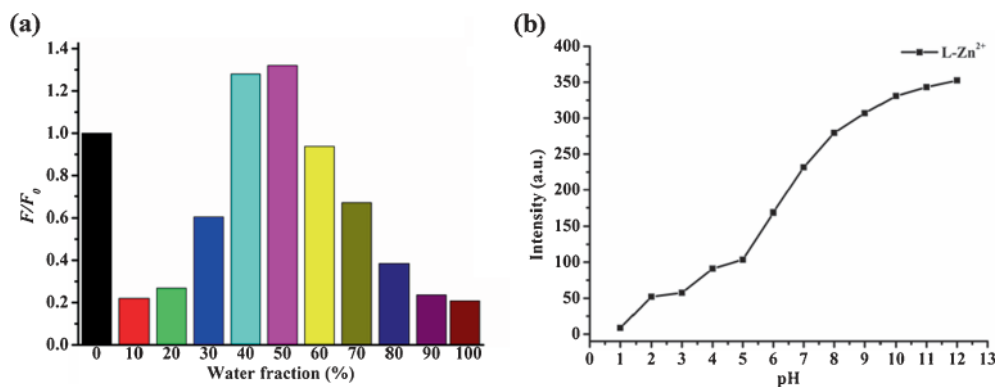
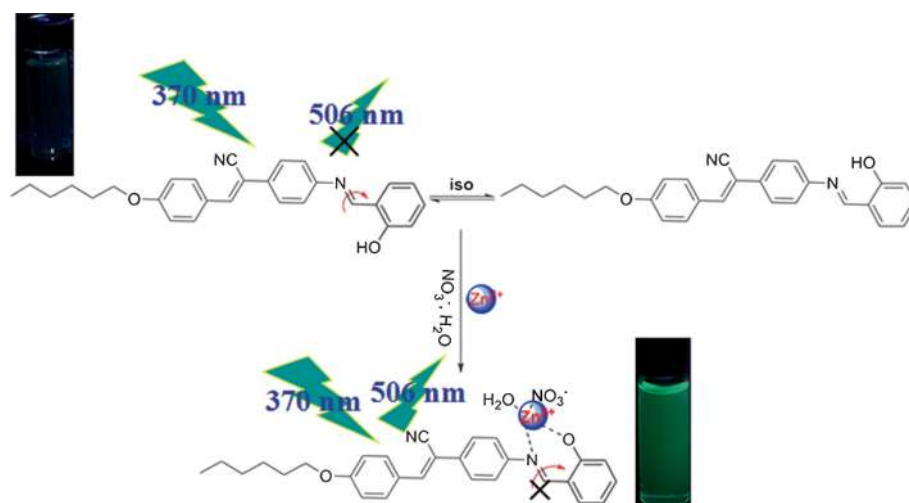


**Figure 7.** (a) Fluorescence response of **L** ( $10 \mu M$ ) towards 1 equiv. of  $Zn^{2+}$  in water/DMF mixed solutions. (b) Plot of fluorescence emission intensity versus pH in DMF/HEPES (1/1, v/v).



### Inhibited isomerization process for the fluorescence emission enhancement

**Scheme 2.** Proposed mechanisms for the fluorescence enhancement of **L** upon the addition of  $\text{Zn}(\text{NO}_3)_2$ .

experiments. In addition, the calculated dihedral angles (table S2) revealed that the structure of **L**- $\text{Zn}^{2+}$  complex is coplanar. From the calculated results, the addition of  $\text{Zn}^{2+}$  to the probe **L** can effectively affect the steric hindrance of the  $\text{C}=\text{N}$  double bond and fix the conjugation system. Such stabilized electronic densities and rigid structure of the complex caused CHEF effect. As a result, an evident enhancement of the fluorescence emission intensity was observed (scheme 2).

## 4. Conclusion

In conclusion, we have successfully synthesized a new kind of  $\alpha$ -cyanostilbene-modified Schiff base **L** as a highly sensitive and selective turn-on fluorescent chemosensor for  $\text{Zn}^{2+}$ . It is worth noting that the fluorescence emission of **L** was not affected by  $\text{Cd}^{2+}$ . We studied the binding model and possible mechanisms for the solvent effect and fluorescence enhancement, and theoretical calculations. On the basis of these results, it is concluded that ICT is an important reason for the red shift of **L** in different solvents. The inhibition of the  $\text{C}=\text{N}$  isomerization caused by complexation with  $\text{Zn}^{2+}$  leads to fluorescence enhancement. The selective  $\text{Zn}^{2+}$  detection property of **L** is so excellent that **L** could serve as an attractive molecular scaffold for highly specific chemosensor for  $\text{Zn}^{2+}$  for potential applications in environmental, biological and medical areas.

## Supplementary Information

Spectral data and calculated electron cloud distribution are given (figures S1–S5 and tables S1 and S2) which can be obtained from [www.ias.ac.in/chemsci](http://www.ias.ac.in/chemsci).

## Acknowledgements

This work was supported by the National Natural Science Foundation of China (21101001 and 61107014), the Natural Science Foundation of Anhui Province (1208085MB21), the 211 Project of Anhui University, and the Team for Scientific Innovation Foundation of Anhui Province (2006KJ007TD).

## References

1. Carter K P, You ng A M and Palmer A E 2014 *Chem. Rev.* doi: 10.1021/cr400546e
2. Liu T and Liu S Y 2011 *Anal. Chem.* **83** 2775
3. Carter R E, Weiss J H and Shuttleworth C W 2010 *Neuroreport* **21** 1060
4. Maret W, Jacob C, Vallee B L and Fisher E H 1999 *Proc. Natl. Acad. Sci.* **96** 1936
5. An J M, Yan M H, Yang Z Y, Li T R and Zhou Q X 2013 *Dyes Pigments* **99** 1
6. Kong L, Chen Y, Ye W B and Zhao L, Song B 2013 *Sens. Actuators B* **177** 218
7. Zhang Y, Guo X F, Zheng L, Jia L H and Qian X H 2013 *J. Photochem. Photobiol. A* **257** 20
8. Liu X J, Zhang N, Zhou J, Chang T J, Fang C L and Shanguan D H 2013 *Analyst* **138** 901
9. Safin D A, Babashkina M G and Garcia Y 2013 *Dalton Trans.* **42** 1969
10. Goswami S, Das A K, Aich K, Manna A, Maity S, Khanra K and Bhattacharyya N 2013 *Analyst* **138** 4593
11. Jiao S Y, Peng L L, Li K, Xie Y M, Ao M Z, Wang X and Yu X Q 2013 *Analyst* **138** 5762
12. Du J, Huang Z, Yu X Q and Pu L 2013 *Chem. Commun.* **49** 5399
13. Mikata Y, Sato Y, Takeuchi S, Kuroda Y, Konno H and Iwatsuki S 2013 *Dalton Trans.* **42** 9688
14. Wang L, Qin W W and Liu W S 2010 *Inorg. Chem. Commun.* **13** 1122

15. Helal A and Kim H S 2013 *Spectrochim. Acta* **105** 273
16. Kumar M, Kumar N and Bhalla V 2013 *Chem. Commun.* **49** 877
17. Ingale S A and Seela F 2012 *J. Org. Chem.* **77** 9352
18. Pearce D A, Jotterand N, Carrico I S and Imperiali B 2001 *J. Am. Chem. Soc.* **123** 5160
19. Zhang Y, Guo X F, Si W X, Jia L H and Qian X H 2008 *Org. Lett.* **10** 473
20. Ding Y B, Xie Y S, Li X, Hill J P, Zhang W B and Zhu W H 2011 *Chem. Commun.* **47** 5431
21. Thirupathi P and Lee K H 2013 *Bioorg. Med. Chem. Lett.* **23** 6811
22. Tong A J, Dong H and Li L D 2002 *Anal. Chim. Acta* **46** 31
23. Xu Z C, Qian X H, Cui J N and Zhang R 2006 *Tetrahedron* **62** 10117
24. Nolan E M and Lippard S J 2004 *Inorg. Chem.* **43** 8310
25. Aoki S, Kagata D, Shiro M, Takeda K and Kimura E 2004 *J. Am. Chem. Soc.* **126** 13377
26. Wang P F, Hong Z R, Xie Z Y, Tong S, Wong O, Lee C S, Wong N, Hung L and Lee S 2003 *Chem. Commun.* 1664
27. Yu T Z, Zhang K, Zhao Y L, Yang C H, Zhang H, Qian L, Fan D W, Dong W K, Chen L L and Qiu Y Q 2008 *Inorg. Chim. Acta* **361** 233
28. Xie Y Z, Shan G G, Li P, Zhou Z Y and Su Z M 2013 *Dyes Pigments* **96** 467
29. Navarro M, Castro W, Martínez A and Delgado R A S 2011 *J. Inorg. Biochem.* **105** 276
30. Mishra A P, Mishra R K and Pandey M D 2011 *Russ. J. Inorg. Chem.* **56** 1757
31. Aziz A A A, Badr I H A and El-Syaed I S A 2012 *Spectrochim. Acta A* **97** 388
32. Wang S C, Men G W, Zhao L Y, Hou Q F and Jiang S M 2010 *Sens. Actuators B* **145** 826
33. Zang L B, Shang H G, Wei D Y and Jiang S M 2013 *Sens. Actuators B* **185** 389
34. Hiseh W H, Wan C F, Liao D J and Wu A T 2012 *Tetrahedron Lett.* **53** 5848
35. Ding C X, He C H and Xie Y S 2013 *Chinese Chem. Lett.* **24** 463
36. Liu S B, Bi C F, Fan Y H, Zhao Y, Zhang P F, Luo Q D and Zhang D M 2011 *Inorg. Chem. Commun.* **14** 1297
37. Hosseini M, Vaezi Z, Ganjali M R, Faridbod F, Abkenar S D, Alizadeh K and Niasari M S 2010 *Spectrochim. Acta A* **5** 978
38. Udhayakumari D, Saravanamoorthy S, Ashok M and Velmathi S 2011 *Tetrahedron Lett.* **52** 4631
39. Paul B K, Kar S and Guchhait N 2011 *J. Photochem. Photobio. A* **220** 153
40. Li H Y, Gao S and Xi Z 2009 *Inorg. Chem. Commun.* **12** 300
41. An B K, Kwon S K, Jung S D and Park S Y 2002 *J. Am. Chem. Soc.* **124** 14410
42. Chung J W, You Y, Huh H S, An B K, Yoon S J, Kim S H, Lee S W and Park S Y 2009 *J. Am. Chem. Soc.* **131** 8163
43. Dou C D, Han L, Zhao S S, Zhang H Y and Wang Y 2011 *J. Phys. Chem. Lett.* **2** 666
44. Zhu L L and Zhao Y L 2013 *J. Mater. Chem. C* **1** 1059
45. Lim C K, Kim S, Kwon I C, Ahn C H and Park S Y 2009 *Chem. Mater.* **21** 5819
46. Jia W B, Yang P, Li J J, Yin Z M, Kong L, Lu H B, Ge Z S, Wu Y Z, Hao X P and Yang J X 2014 *Poly. Chem.* **5** 2282
47. Jia W B, Wang H W, Yang L M, Lu H B, Kong L, Tian Y P, Tao X T and Yang J X 2013 *J. Mater. Chem. C* **1** 7092
48. Gou C, Qin S H, Wu H Q, Wang Y, Luo J and Liu X Y 2011 *Inorg. Chem. Commun.* **14** 1622
49. Kim B, Yeom H R, Choi W Y, Kim J Y and Yang C 2012 *Tetrahedron* **68** 6696
50. Lu H B, Qiu L Z, Zhang G Y, Ding A X, Xu W B, Zhang G B, Wang X H, Kong L, Tian Y P and Yang J X 2014 *J. Mater. Chem. C* **2** 1386
51. Frisch M J G W T, Schlegel H B, Scuseria G E, Robb M A, Cheeseman J R, Scalmani G, Barone V, Mennucci B, Petersson G A, Nakatsuji H, Caricato M, Li X, Hratchian H P, Izmaylov A F, Bloino J, Zheng G J, Sonnenberg L, Hada M, Ehara M, Toyota K, Fukuda R, Hasegawa J, Ishida M, Nakajima T, Honda Y, Kitao O, Nakai H, Vreven T, Montgomery J A, Peralta Jr J E, Ogliaro F, Bearpark M, Heyd J J, Brothers E, Kudin K N, Staroverov V N, Kobayashi R, Normand J, Raghavachari K, Rendell A, Burant J C, Iyengar S, Tomasi S J, Cossi M, Rega N, Millam J M, Klene M, Knox J E, Cross J B, Bakken V, Adamo C, Jaramillo J, Gomperts R, Stratmann R E, Yazyev O, Austin A J, Cammi R, Pomelli C, Ochterski J W, Martin R L, Morokuma K, Zakrzewski V G, Voth G A, Salvador P, Dannenberg J J, Dapprich S, Daniels A D, Farkas O, Foresman J B, Ortiz J V and Cioslowski J, Fox D J *Gaussian 09, Revision B. 01*. Gaussian, Inc., Wallingford CT. 2009